processes

MDPI

Review

Preparation, Modification, and Application of Graphitic Carbon Nitride in Photocatalytic Degradation of Antibiotics

Xiaoning Lu, Mingchao Zhu *, Dongdong Chen, Jiayang Wu, Shuangqian Gao, Yimin Zhao, Junling Yang, Shuping Li and Jiang Meng *

Key Laboratory of Water Safety and Aquatic Ecosystem Health of Xizang Autonomous Region, Xizang Minzu University, Xianyang 712082, China; luxiaoning001@126.com (X.L.); ddchen@xzmu.edu.cn (D.C.); 15235553748@163.com (J.W.); 13934814252@163.com (S.G.); zym2100229727@163.com (Y.Z.); lishuping@xzmu.edu.cn (S.L.)

* Correspondence: mczhu@xzmu.edu.cn (M.Z.); mengjiang@xzmu.edu.cn (J.M.)

Abstract

This review addresses the environmental and health risks caused by antibiotic abuse, focusing on the inefficiency of traditional treatment methods and their tendency to cause secondary pollution, as well as the limitations of g-C_3N_4 in photocatalytic antibiotic degradation, such as insufficient visible light utilization and high carrier recombination rates. It systematically summarizes modification strategies and application advances of g-C_3N_4. Compared with previous reviews on carbon nitride, this work distinguishes itself by precisely targeting the cutting-edge application scenario of antibiotic-specific degradation, providing an in-depth analysis of how precursor selection and preparation methods regulate material properties, and emphasizing the role of modification approaches—including crystal optimization, element doping, surface modification, and heterojunction construction—in enhancing catalytic efficiency. It offers targeted and forward-looking insights for the practical application of this material in controlling antibiotic pollution in complex water environments.

Keywords: graphitic carbon nitride; antibiotic degradation; photocatalysis; modification strategies

check for updates

Academic Editors: Maria Alejandra Ayude and Lucila Inés Doumic

Received: 10 September 2025
Revised: 9 October 2025
Accepted: 10 October 2025
Published: 21 October 2025

Citation: Lu, X.; Zhu, M.; Chen, D.; Wu, J.; Gao, S.; Zhao, Y.; Yang, J.; Li, S.; Meng, J. Preparation, Modification, and Application of Graphitic Carbon Nitride in Photocatalytic Degradation of Antibiotics. *Processes* **2025**, *13*, 3365. https://doi.org/10.3390/pr13103365

Copyright: © 2025 by the authors. Licensee MDPI, Basel, Switzerland. This article is an open access article distributed under the terms and conditions of the Creative Commons Attribution (CC BY) license (https://creativecommons.org/licenses/by/4.0/).

1. Introduction

In contemporary society, the widespread use of antibiotics has brought numerous benefits, but their abuse in medical and agricultural fields has led to antibiotics entering the environment through wastewater, agricultural runoff, and medical waste. These antibiotics are resistant to natural degradation, persist in the environment, and form a vicious cycle through bioaccumulation, further contributing to the emergence and global spread of antibiotic resistance, which has become one of the most severe challenges in environmental protection [1]. Currently, common methods for treating antibiotics include biodegradation, physical adsorption, and advanced oxidation technologies. Biodegradation utilizes microorganisms in activated sludge to decompose antibiotics into non-toxic or low-toxicity small molecules. However, because antibiotics have an inhibitory effect on microorganisms, this method is not suitable for treating wastewater with high concentrations of antibiotics [2]. Physical adsorption methods utilize the surface adsorption properties of materials (such as activated carbon or clay) to rapidly adsorb antibiotic molecules from aqueous solutions onto solid surfaces, thereby achieving removal. However, this approach exhibits significant limitations: its adsorption capacity is limited (typically ranging from 50 to 500 mg/g), and

saturated adsorbents are prone to desorption, failing to fundamentally eliminate antibiotics. Moreover, improper disposal of spent adsorbents may lead to secondary pollution [3]. Advanced oxidation methods generate hydroxyl radicals (·OH), superoxide radicals ($\cdot O_2^-$), and other radicals through various means. These radicals have extremely high oxidative capacities, allowing them to effectively attack antibiotic molecules, leading to structural damage and degradation. Common advanced oxidation methods include photocatalysis, ozonation, Fenton reaction, and ultrasonic treatment [4,5]. Photocatalysis is an efficient and sustainable advanced oxidation technology with significant research and application value in wastewater treatment [6]. Graphitic carbon nitride (g-C_3N_4) exhibits promising application prospects in the field of photocatalysis due to its stable physicochemical properties, suitable bandgap, and ease of preparation. Under visible light irradiation, g-C_3N_4 generates photogenerated electron-hole pairs. The electrons react with water and dissolved oxygen in water to produce oxidative radicals. These radicals, along with the holes generated by g-C_3N_4, participate in redox reactions with antibiotics, converting them into non-toxic or low-toxicity small molecules, thereby reducing antibiotic pollution in the environment [7].

In summary, this paper first introduces the basic structure of graphitic carbon nitride and the fundamental principles of its photocatalytic degradation of antibiotics. It summarizes the effects of different types of precursors on the morphology of carbon nitride and the influence of various preparation methods on its functionality. Additionally, it explores four modification methods—crystal structure optimization, element doping, surface modification, and the construction of heterojunctions—to enhance the photocatalytic efficiency of g-C_3N_4. The paper provides further research suggestions to improve the photocatalytic efficiency of g-C_3N_4 and refine the modification methods.

2. The Structure of Graphitic Carbon Nitride and the Mechanism of Photocatalytic Degradation of Antibiotics

2.1. The Basic Structure of Graphitic Carbon Nitride

Triazine rings (C_3N_3) and heptazine rings (C_6N_7) are considered the two ideal fundamental structural units of g-C_3N_4. After density functional theory (DFT) calculations, it has been found that the g-C_3N_4 composed of C_6N_7 has a lower thermodynamic energy and a more stable structure. Therefore, C_6N_7 is currently widely regarded as the fundamental structural unit of g-C_3N_4. In the heptazine ring, the carbon and nitrogen atoms are all sp^2 hybridized and connected by σ bonds. The heptazine rings are interconnected through nitrogen atoms, forming outward-extending layers, which are connected by van der Waals forces [8]. It forms a layered stacking structure similar to graphite.

Graphitic carbon nitride possesses unique physicochemical properties. These properties stem from its graphite-like lattice morphology, high degree of polymerization, and heptazine ring structure. The layered structure of g-C_3N_4, similar to that of graphite, imparts good light absorption capacity and electronic conductivity [9]; A high degree of polymerization indicates a greater degree of cross-linking in the molecular chains, enhancing its durability in catalytic and other applications. The heptazine ring structure endows g-C_3N_4 with excellent thermal and chemical stability, allowing it to maintain structural integrity under high-temperature conditions while demonstrating good tolerance in strong acid or strong alkali environments. These characteristics enable g-C_3N_4 to retain catalytic activity under extreme conditions. Strong covalent bonds and van der Waals forces between molecules render g-C_3N_4 insoluble in common solvents [10]. Compared to soluble catalysts, the separation and reuse of g-C_3N_4 is more convenient, which helps reduce costs and improve the economic efficiency of the reaction. The excellent physicochemical properties of graphitic carbon nitride make it an ideal, environmentally friendly photocatalytic material, especially demonstrating broad application prospects in the degradation of antibiotics.

2.2. The Mechanism of Photocatalytic Degradation of Antibiotics by Graphitic Carbon Nitride

Behzad Moeinifard et al. [11] performed UV-Vis diffuse reflectance spectroscopy (UV-Vis DRS) on graphitic carbon nitride. Using the Kubelka-Munk function, the band gap (Eg) of the carbon nitride was determined to be 2.64 eV, indicating that graphitic carbon nitride can absorb visible light with wavelengths shorter than 460 nm [11]. Under visible light irradiation, photogenerated electron-hole pairs can be produced. According to band theory, semiconductor materials consist of a valence band (VB) and a conduction band (CB), with the intermediate region that lacks electrons referred to as the bandgap width (E_h). When a semiconductor absorbs photons with energy exceeding E_h, electrons in the valence band transition to the conduction band, thereby forming electron-hole pairs and triggering catalytic reactions. High-crystalline g-C_3N_4 photocatalysts: Synthesis, structure modulation, and H-evolution application [12].

The semiconductor properties enable effective light energy absorption. As shown in Figure 1, when g-C_3N_4 is illuminated with light of a wavelength greater than the bandgap width, electrons in the valence band are excited to the conduction band, generating photogenerated electrons (e^-) and holes (h^+). The photogenerated electrons and holes migrate within the g-C_3N_4 lattice and reach the surface, where the electron-hole pairs can react with water molecules and dissolved oxygen to produce hydroxyl radicals (·OH) and superoxide anions ($\cdot O_2^-$). These highly oxidative reactive species can react with the double bonds or aromatic rings in antibiotic molecules, degrading the antibiotics into small molecules such as CO_2 and H_2O [13]. The holes generated in the valence band of the catalyst are also strong oxidants, and some of these holes can react with various functional groups in the antibiotic molecules, thereby degrading the large antibiotic molecules into smaller ones.

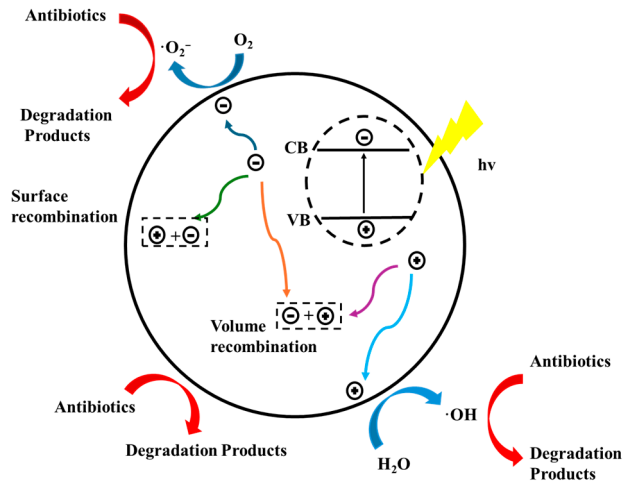

Figure 1. The principle of graphitic carbon nitride photocatalytic antibiotic degradation.

The core of using g-C_3N_4 as a photocatalyst for the degradation of antibiotics lies in the rapid generation of photogenerated electrons and the efficient separation of charges. Therefore, researchers have proposed various methods to optimize the photocatalytic performance of g-C_3N_4.

3. The Influence of Graphitic Carbon Nitride Precursors on Antibiotic Degradation

Carbon nitride crystals have not yet been found in nature, and all existing carbon nitride materials are synthetically produced. Graphitic carbon nitride is typically obtained by polymerizing one or more nitrogen-rich organic compounds containing C-N bonds.

Different precursors result in variations in the reaction processes and conditions during the synthesis of carbon nitride, leading to differences in reaction rates and processes, which ultimately affect the properties of the final products [14]. When pursuing the performance and cost-effectiveness of materials, it is essential to choose appropriate preparation methods while considering specific application requirements and experimental conditions.

The g-C_3N_4 is formed through polymerization reactions between precursor molecules, resulting in a layered graphite-like structure. Commonly used precursors include urea, melamine, thiourea, and cyanamide. The molecular structure of the precursors determines the microstructure of the carbon nitride [15]. For example, melamine can form layered graphitic carbon nitride upon pyrolysis, while the carbon nitride generated from urea pyrolysis typically exhibits a micrometer-sized sheet-like morphology. Carbon nitride derived from thiourea pyrolysis exhibits a sheet-like structure with high specific surface area. During the synthesis of carbon nitride from cyanamide, the evolved gases cause collapse and dense stacking between layers, which restricts pore formation and results in a relatively low specific surface area. Graphitic carbon nitride prepared from a mixture of various precursors may result in more ordered or complex structures [16]. The g-C_3N_4 with different morphological structures exhibits varying light absorption capabilities and electron-hole generation rates, which in turn affect its ability to photocatalytically degrade antibiotics. The characteristics of different precursors used to prepare carbon nitride are shown in Table 1.

Table 1. Characteristics of carbon nitride prepared by different precursors.

Precursor	Preparation Process and Structure Morphology	Performance Characteristics
Urea	Pyrolysis at 500–600 °C produces a dispersed sheet structure with high porosity.	Specific surface area (BET) typically ranging from 60 to 100 m^2/g, a band gap of approximately 2.7 eV [17].
Melamine	Pyrolysis above 500 °C yields a dense and bulky block-like morphology with an internally ordered layered structure.	Exhibits good crystallinity, demonstrates an ordered layered structure, and possesses a band gap of approximately 2.7 eV [18].
Thiourea	Thiourea pyrolysis at 550–650 °C yields porous sheet-like architectures.	Sulfur doping effectively narrows the bandgap and enhances visible light absorption [19].
Cyanamide	Copyrolysis at 500 °C results in amorphous bulk-aggregated morphology.	It exhibits an amorphous bulk-aggregated morphology with low specific surface area and a band gap of approximately 2.7 eV [20].

4. The Influence of Different Preparation Methods on the Degradation of Antibiotics by Graphitic Carbon Nitride

The synthesis methods of graphitic carbon nitride mainly include thermal condensation, solvothermal method, template method, sol–gel method, and high-energy microwave method [21–25]. Each method has different reaction principles and conditions, resulting in variations in characteristics such as porosity, specific surface area, and crystallinity of the carbon nitride materials. Here (Table 2), we summarize the advantages and disadvantages of different preparation methods.

Thermal condensation is a commonly used method for preparing g-C_3N_4, typically utilizing nitrogen-rich precursors such as urea and melamine. Under high-temperature conditions, the precursors undergo condensation reactions to form carbon nitride. This method effectively removes impurities and improves the crystallinity and purity of the material. The suitable pyrolysis temperature range for the precursors varies; higher temperatures help eliminate impurities and enhance crystallinity, but excessively high temperatures may damage the material structure [26]. It typically starts to lose weight significantly at 500–600 °C and is almost completely decomposed at around 650 °C. Sulakshana et al. [27]

used $CoNiO_2$ as a substrate for the growth of g-C_3N_4 and prepared a highly crystalline g-C_3N_4 with stability through the thermal condensation method. After four consecutive cycles, the efficiency decreased moderately by 8%, confirming its stability in the photocatalytic degradation of tetracycline.

The solvothermal method involves dissolving precursors in a suitable solvent and reacting them under high temperature and pressure conditions in a sealed reaction vessel. The advantage of this method is that it allows for control over the reaction environment, enabling the adjustment of the morphology and particle size of carbon nitride, which in turn affects its specific surface area and catalytic performance. By selecting different solvents and reaction times, carbon nitride materials with varying structures can be obtained. Zhou et al. [28] employed a formic acid-assisted hydrothermal method to prepare nitrogen-deficient carbon nitride, which was utilized for the photocatalytic degradation of tetracycline. In the experiment, a beaker was filled with 100 mL of TC-HCl solution (10 mg/L) at pH 5.3. Then, 50 mg of the catalyst was added to the solution, achieving a degradation rate of 95.1% within 60 min.

The template method utilizes the structure of template materials to guide the morphology and porosity of carbon nitride. By depositing precursors onto the template and then removing the template, carbon nitride materials with specific shapes and pore structures can be obtained [29]. This method effectively enhances the specific surface area and catalytic performance of the materials and is suitable for preparing nanoscale carbon nitride. Wu et al. [30] used melamine as the precursor and ammonium chloride as a gas template agent to prepare coral-like g-C_3N_4 (PCN) with porous nitrogen vacancies. PCN achieved degradation efficiencies of 80–100% for sulfanilamide and chain sulfanilamide within 120 min, and 40–70% for sulfamethoxazole. Compared to bulk carbon nitride, coral-like g-C_3N_4 has a larger specific surface area and higher electron-hole transfer efficiency, thus exhibiting superior antibiotic degradation capabilities.

The sol–gel method is a wet chemical synthesis technique that involves forming a sol, which subsequently transforms into a gel, ultimately yielding carbon nitride materials. This method offers the advantage of low-temperature synthesis, helping to avoid structural damage to the materials caused by high temperatures. Additionally, the sol–gel method allows for the preparation of carbon nitride in a relatively short time, enhancing production efficiency.

The high-energy microwave method utilizes the energy provided by microwave radiation to promote reactions, enabling the rapid synthesis of carbon nitride [31]. This method features uniform heating and short reaction times, effectively improving the purity and performance of the materials. By adjusting the microwave power and reaction time, carbon nitride materials with different properties can be obtained. Li et al. [32] experimentally demonstrated that increasing the microwave power helps optimize the morphology of carbon nitride and enlarge its specific surface area, thereby exposing more active sites. The expanded specific surface area concurrently enhances light transmittance. The g-C_3N_4 samples prepared at microwave powers of 30 W, 40 W, and 50 W exhibited bandgap energies of 2.67 eV, 2.61 eV, and 2.58 eV, respectively. The slight narrowing of the bandgap suggests that microwave regulation influences the precursor's structure, which subsequently modifies the electronic structure of g-C_3N_4. This alteration is conducive to improving the material's light absorption performance [32].

Table 2. Comparison of Advantages and Disadvantages of Different Methods for Preparing Carbonitride [32–36].

Name	Principle of Preparation	Typical Product Characteristics	Scalability	Conclusion
Thermal Condensation Method	Carbon nitride is obtained by directly condensing nitrogen-rich precursors under high temperature in an air or inert gas atmosphere.	High crystallinity, but very low specific surface area (<10 m^2/g), bulk morphology.	The process is simple, easily scalable to the kilogram level, and demonstrates excellent scalability.	Its low specific surface area severely limits the number of active sites, resulting in low intrinsic catalytic efficiency. Subsequent exfoliation or acid treatment is often required, which increases overall complexity and cost.
Solvothermal Method	The precursor is dissolved in a heat-conducting medium, and the mixed solution is placed in a high-pressure reaction kettle to prepare carbon nitride under specific temperature and pressure conditions.	Controllable morphology (nanosheets, microspheres), good dispersion, medium specific surface area.	Safety risks associated with high-pressure environments and the batch processing mode are major bottlenecks for scale-up production, resulting in poor scalability.	The high time cost and capital investment are traded for better morphology control. Its "mild" conditions come at the cost of sacrificing production efficiency and throughput; cost-effectiveness is a primary concern.
Template Method	The structure of the template material is used to guide the morphology and characteristics of carbon nitride.	Very high specific surface area (>100 m^2/g), tunable pore structure.	The template removal step poses significant environmental issues and incurs additional purification costs, resulting in moderate scalability.	Performance enhancement comes at the cost of complex processes, high cost, and environmental unfriendliness.
Sol–Gel Method	A colloid (sol) is formed in the solution, which is then converted into solid material through drying and heat treatment.	High purity, homogeneous composition, medium to high specific surface area.	Shrinkage and cracking issues during the drying process are difficult to control at scale, adversely affecting product consistency and resulting in moderate scalability.	The advantage of "lower temperature" is often offset by expensive precursors and long process times. Low cost-effectiveness; more suitable for lab-scale preparation of materials requiring special purity.
High-Energy Microwave Method	Rapid heating of materials is achieved through microwave irradiation.	Rapid nucleation often leads to non-uniform crystallinity, easily forms ultra-thin nanosheets, nanorods, spheres, and other morphologies.	The process is characterized by poor reaction controllability and low yield, thus limited to small-scale laboratory preparation.	Despite outstanding time and energy efficiency, the fatal flaws of low yield and difficulty in scaling up currently prevent its application in actual production.

5. The Influence of Modification Methods of Graphitic Carbon Nitride on Antibiotic Degradation

g-C_3N_4 has several issues, including a small specific surface area, insufficient absorption efficiency for visible light, and a tendency for photogenerated electron-hole pairs to recombine. These problems limit the practical application of g-C_3N_4 in the photocatalytic degradation of antibiotics. Therefore, researchers have focused on optimizing the material's band structure to extend its response range to visible light and enhance its light absorption capacity; altering the electronic structure to promote the generation and separation of electron-hole pairs; and increasing the migration pathways for electrons and holes to reduce the probability of recombination [37]. By enhancing the photocatalytic ability of g-C_3N_4 through the aforementioned approaches, the goal of efficiently degrading antibiotics can be achieved. Common methods include crystal optimization, element doping, surface modification, and the construction of heterojunctions. These methods are expected to improve the photocatalytic performance of g-C_3N_4, facilitating its practical application in the degradation of antibiotics. Here (Table 3), we summarize the different optimization methods.

Table 3. Different Optimization Methods [38–41].

Optimization Method	Description	Main Advantages	Exemplary Studies
Crystal Structure Optimization	Morphology control to increase specific surface area and reduce defects	Improved photocatalytic performance and enhanced electron-hole transport efficiency	The prepared crystalline polymeric carbon nitride (CCN) with an ultrathin two-dimensional nanosheet structure efficiently removes various high-concentration organic pollutants (50 mg·L^{-1}) and achieves synergistic removal of organic contaminants and heavy metal ions. Within 40 min, the removal rate for all organic pollutants—including antibiotics and dyes—exceeds 95%.
Element Doping	Doping with metals and non-metals to adjust the band structure and create impurity levels	Expanded light absorption range and reduced recombination rate of photogenerated electron-hole pairs	A series of Bi/Ce/g-C_3N_4 photocatalysts with different doping ratios were prepared by direct calcination and applied for the photocatalytic degradation of Rhodamine B (RhB) and sulfamethoxazole (SMX). Experimental results demonstrated that the photocatalytic performance of Bi/Ce/g-C_3N_4 surpassed that of single-component samples. Under optimal conditions, the degradation rates of RhB (20 min) and SMX (120 min) by Bi/Ce/g-C_3N_4 reached 98.3% and 70.5%, respectively.
Surface Modification	Optimizing electronic structure through noble metal deposition and molecular/ionic modification	Increased light absorption capacity and facilitated rapid separation of electron-hole pairs	A metal-free composite photocatalyst comprising zero-dimensional (0D) graphene quantum dots (GQDs) decorated graphitic carbon nitride nanorods (g-CNNR) was successfully prepared via a hydrothermal method. Physicochemical characterization revealed that the GQDs/g-CNNR photocatalyst exhibits high crystallinity, enhanced visible-light absorption, and a staggered band alignment, which collectively facilitate the generation, migration, and separation of photoinduced electrons and holes. These advantages contribute to the significantly improved photocatalytic activity of GQDs/g-CNNR for efficient antibiotic degradation. Its photocatalytic reaction rate is 3.46 and 2.03 times higher than that of g-C_3N_4.
Heterojunction Construction	Combining different semiconductors to form heterostructures that reduce electron-hole recombination	Enhanced photoelectric conversion efficiency and extended spectral response range	A non-metallic heterojunction composite photocatalyst (H-g-C_3N_4/BPQDs) was synthesized using g-C_3N_4 and black phosphorus quantum dots (BPQDs) as raw materials through a process involving hydrothermal impregnation, high-temperature calcination, and ice-assisted ultrasonication. The obtained H-g-C_3N_4/BPQDs were applied for the removal of antibiotics and biofouling from water under visible-light irradiation. Owing to the porous structure and high specific surface area of H-g-C_3N_4, the resulting Type II heterojunction structure enhanced visible-light absorption, accelerated interfacial charge transfer, and suppressed the recombination of photogenerated electron-hole pairs. Under visible-light irradiation, the degradation efficiency of H-g-C_3N_4/BPQDs for tetracycline (TC) exceeded 91% within 30 min.

5.1. Crystal Structure Optimization

Crystal structure optimization is divided into morphology control and vacancy introduction. Morphology control includes porosification and dimensional reduction. Porosification aims to increase the specific surface area of the catalyst, exposing more active sites, while dimensional reduction enhances the light absorption capability of carbon nitride by nanostructuring in specific directions, improving crystallinity, and shortening the distance for photogenerated electrons and holes to migrate to the catalyst surface, thereby enhancing photocatalytic performance [42]. Common special morphologies include nanosheets, nanotubes, nanoparticles, nanobubbles, and other porous structures [43].

Dhruti Sundar Pattanayak et al. [44] The effectiveness and simplicity of thermally exfoliated g-C_3N_4 for the degradation of tetracycline hydrochloride (TCH) under sunlight were demonstrated. This study investigated the thermal exfoliation of thiourea-derived g-C_3N_4 at temperatures of 450, 475, 500, 525, and 550 °C. At a catalyst dosage of 0.4 g/L, approximately 71% of TCH (initial concentration: 10 mg/L) was degraded after 60 min of direct sunlight exposure. Results indicated a TOC removal rate of 69% for the 10 mg/L TCH solution over 60 min, which aligns well with the degradation efficiency. The degradation process followed pseudo-first-order kinetics, with a rate constant of 0.020 min^{-1} (R^2 = 0.997).

The introduction of vacancies can enhance the adsorption and activation ability of carbon nitride for dissolved oxygen, thereby increasing the rate of photocatalytic reactions.

Zhan et al. [45] combined thermal calcination and hydrothermal processes to design nitrogen vacancies and oxygen substitution for the co-modification of coral-like carbon nitride. The results confirmed that nitrogen vacancies extended the adsorption edge into the visible light region, hindering the recombination of photogenerated electron-hole pairs, while oxygen substitution accelerated surface/interface kinetics. Consequently, this catalyst was able to degrade 80% of tetracycline, with a pseudo-first-order kinetic constant of 0.124 min^{-1}, which is 13.8 times higher than that of the original carbon nitride.

5.2. Element Doping

The principle of element doping to modify g-C_3N_4 is to enhance the photocatalytic ability of the catalyst by altering its electronic properties and optical/electrical characteristics. For example, when metal ions (e.g., Fe, Cu, K) are doped into the structural units of g-C_3N_4, donor or acceptor energy levels are generated above the valence band or below the conduction band, leading to a narrowing of the bandgap and an expansion of the light absorption range [46] In contrast, non-metal element doping involves substituting N, C, or H atoms in g-C_3N_4, creating lattice defects that act as traps for photogenerated electrons or holes. This process reduces the recombination rate of electron-hole pairs, thereby enhancing the photocatalytic ability of g-C_3N_4 [47,48]. Zeng et al. [49] prepared a visible light-driven Co and Gd co-doped three-dimensional porous graphitic carbon nitride, which demonstrated a high degradation ability for ciprofloxacin under low-power lamp irradiation. Under visible light irradiation, approximately 21.2%, 55.8%, 67.4%, and 85% of CIP was degraded after 150 min of exposure to CN, Co-CN, Gd-CN, and $Gd_{0.12}Co_{0.05}$/CN, respectively. The results demonstrate that the incorporation of photocatalysts significantly enhances the CIP removal efficiency. The enhanced photocatalytic activity is primarily attributed to the doping of Gd and Co, which increased the specific surface area of g-C_3N_4, providing more reactive sites. Additionally, the introduction of Gd and Co improved the band structure, narrowing the bandgap of the semiconductor catalyst, facilitating charge separation, and enhancing the adsorption and activation capacity for dissolved oxygen in water.

5.3. Surface Modification

The principle of surface modification is based on optimizing the light absorption capability of g-C_3N_4 and enhancing charge carrier separation. Surface modification methods, such as noble metal deposition, carbon-based material modification, and molecular grafting, can narrow the bandgap of g-C_3N_4 and increase its visible light absorption range [50,51]. The noble metal ions (e.g., Ag) used to modify g-C_3N_4 can effectively suppress the recombination of electron-hole pairs, increasing the density of photogenerated charge carriers and enhancing the photocatalytic activity of g-C_3N_4. Jiamin Gan et al. [52] designed gold nanoparticles (Au NPs) to overcome these drawbacks via their localized surface plasmon resonance, thereby enhancing the light absorption of g-C_3N_4. Research demonstrated that the introduction of Au NPs improved the photoelectrochemical performance of g-C_3N_4 under illumination, leading to a high yield of reactive oxygen species (ROS) and exceptional efficacy in degrading tetracycline hydrochloride. Zhao Yue et al. [53] fabricated an innovative photocatalyst by implanting zero-dimensional carbon quantum dots (CQD) in dimensional C_3N_4 nanorods. The combination of CQD accelerates charge separation/transfer and broadens the light-harvesting ability through conversion of fluorescence properties at the same time. The CQDs/g-C_3N_4 catalyst exhibits excellent photocatalytic degradation performance under visible-light irradiation, with a removal rate of 94.3% for tetracycline, which is 1.2 times that of the pure g-C_3N_4 catalyst.

5.4. Constructing Heterojunctions

Constructing heterojunctions can accelerate the migration and separation of photogenerated electron-hole pairs. Additionally, the introduction of other catalytic components can expand the visible light response range of g-C_3N_4 and improve its absorption and utilization efficiency, significantly enhancing the photocatalytic performance of the composite catalyst. The construction of an internal electric field (IEF) has been demonstrated as an effective strategy to enhance charge separation and migration efficiency. Heterojunctions such as Type-II, Z-scheme, S-scheme, and Schottky junctions can form an IEF through band alignment, thereby promoting charge separation [54]. Depending on the band structures of the different semiconductors in the composite, the formed heterojunctions can be roughly categorized into four types: Type I, Type II, Type III, and Z-type heterojunctions.

Type I heterojunctions are formed by combining two semiconductor materials with different band structures. As shown in Figure 2a, the conduction and valence bands of the two photocatalysts overlap in a continuous energy range. This overlap allows electrons and holes to accumulate in the same region. Due to the differing work functions of the semiconductor materials, an internal electric field is generated at the interface. The presence of this internal electric field significantly enhances the separation efficiency of photogenerated electrons and holes, reducing the probability of their recombination [55,56].

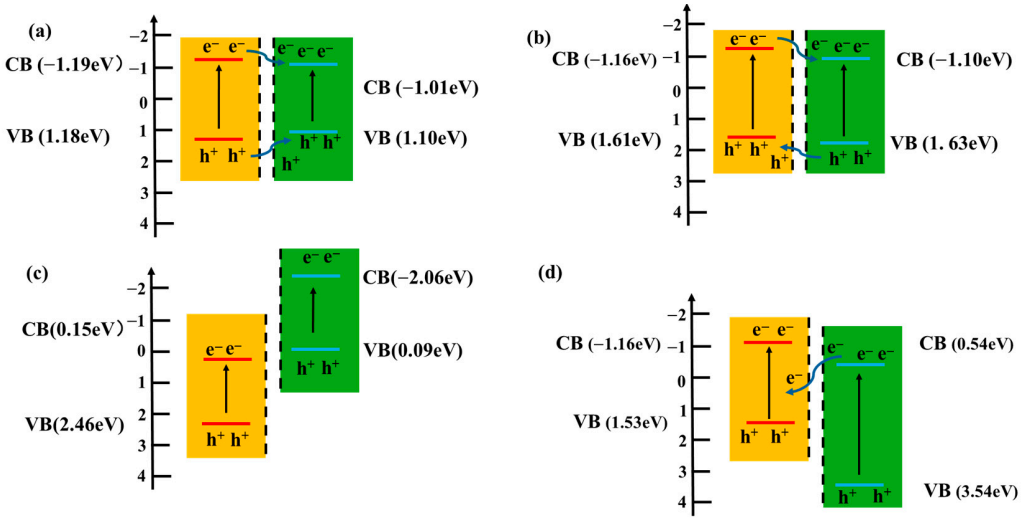

Figure 2. Schematic diagram of (**a**) type I.heterojunctions, (**b**) type II. heterojunctions, (**c**) type III. heterojunction and (**d**) type Z heterojunctions [57–59].

Type II heterojunctions, as shown in Figure 2b, are characterized by the conduction band of one material being lower than the valence band of another material, creating a natural separation point for electrons and holes. This mechanism allows photogenerated electrons and holes to be spatially separated, distributed across the two materials, thus forming a potential difference. Since the bottom of the conduction band and the top of the valence band are located in two different materials, electrons accumulate on the side with the lower conduction band, while holes concentrate on the side with the higher valence band. Type II heterojunctions effectively reduce the recombination probability of electron-hole pairs, thereby enhancing photocatalytic efficiency.

Type III heterojunctions, as shown in Figure 2c, are characterized by the absence of overlapping regions in the conduction and valence bands of the two semiconductors, which reduces the recombination pathways for electron-hole pairs and lowers the probability of recombination. Since the conduction and valence bands are not located within the same material, electrons and holes naturally tend to distribute themselves across the two different materials, leading to quantum tunneling effects.

Type Z heterojunctions, as shown in Figure 2d, primarily rely on the synergistic effects between two semiconductor materials. The energy bands of the two materials connect in the Z-type heterojunction, creating effective energy separation and transfer pathways. This arrangement allows for efficient separation of photogenerated electrons and holes in different semiconductor materials, reducing the likelihood of recombination [60]. Additionally, Z-type heterojunctions enhance charge mobility, thereby improving reaction efficiency [61]. Furthermore, the energy band structure of the two semiconductor materials in the Z-type heterojunction can create an internal electric field, which accelerates the separation of electrons and holes, further enhancing photocatalytic efficiency. Lastly, the different light absorption characteristics of the semiconductor materials enable the Z-type heterojunction to effectively utilize a broader spectrum of light, improving the overall efficiency of photocatalysis.

Currently, Z-type heterojunction catalysts constructed with various materials have shown extensive research and application potential in the photocatalytic degradation of antibiotics. A key area of focus is the development of reusable photocatalysts. Z-type heterojunction materials formed by g-C_3N_4 and magnetic materials demonstrate good chemical stability and durability during reactions, maintaining their photocatalytic performance even after multiple cycles [62]. In terms of applications, Z-type heterojunction catalysts involving g-C_3N_4 have achieved promising results in the degradation of different types of antibiotics. For instance, Zhang et al. [63] utilized an impregnation method to construct a TiO_2/g-C_3N_4 heterojunction, enhancing the generation and migration capabilities of photogenerated charge carriers. Experiments indicated that under conditions of 0.7 g/L catalyst dosage and 2 h of visible light irradiation, the TiO_2/g-C_3N_4 heterojunction achieved a tetracycline removal rate of 94.64%. The effective separation and transfer of charges contribute to improved reaction kinetics in photocatalytic processes. The incorporation of TiO_2 broadens the light absorption range, allowing the composite catalyst to utilize a wider spectrum of light, especially in the visible range, thereby enhancing the material's ability to photocatalytically degrade antibiotics.

6. Future Development Trends of Graphitic Carbon Nitride

6.1. Application in Environmental Engineering

Constructed wetlands, as an eco-friendly and cost-effective wastewater treatment technology, are widely used for treating domestic sewage, agricultural runoff, and lightly contaminated industrial effluents. Their core purification principle relies on the synergistic interactions among plants, microorganisms, and the substrate (filter media). In recent years, introducing the g-C_3N_4 into the substrate of constructed wetlands has provided an innovative and promising direction for enhancing pollution treatment efficiency, particularly for the removal of recalcitrant organic pollutants. Haidong Zhou et al. [64] constructed a novel photocatalytic bionic system (PCBS) by integrating artificial aquatic plants (AquaMats) with photocatalysts (g-C_3N_4 and TiO_2). The results indicated that the optimal loading amount for both photocatalysts on the artificial aquatic plants was 8.25 g/m^2. The total removal rates of antibiotics ranged from 21.2% to 64.4%, while the removal rates of antibiotic resistance genes (ARGs) varied from 0.7% to 28.1% in sediments and from 1.0% to 65.9% in the water phase of the PCBS.

Pilot-scale systems, serving as a critical bridge connecting laboratory research and industrial application, are widely used to validate the feasibility and stability of new processes and materials under real operating conditions. Their core value lies in simulating long-term operation in realistic environments to obtain essential process parameters and design basis for scale-up. In recent years, evaluating the performance of g-C_3N_4 modified materials within pilot-scale systems has provided a reliable and necessary platform for

validating the transition of this material from theoretical research to practical water treatment engineering. Ilaeira Rapti et al. [65] conducted experiments using real wastewater samples collected from the secondary effluent of a hospital wastewater treatment plant (WWTP), with drug concentrations in the samples at peak and inherent levels. The g-C_3N_4 and 1% MoS_2/g-C_3N_4 (1MSCN) were used as photocatalytic materials. The photocatalytic experiments were carried out in a lab-scale pilot setup consisting of a stainless-steel lamp reactor (46 L) equipped with ten UVA lamps and a quartz filter connected in series to a polypropylene recirculation tank (55–100 L). Additionally, experiments were conducted using a solar simulator apparatus (Atlas Suntest XLS+) at an irradiation intensity of 500 W/m^2. The 1MSCN composite consistently demonstrated higher photocatalytic performance than g-C_3N_4. The removal rates of pharmaceutical compounds using g-C_3N_4 and 1MSCN were 30% and 54% higher, respectively.

6.2. Machine Learning-Assisted Design of g-C_3N_4 Materials

The g-C_3N_4 as a tunable photocatalytic material, exhibits a complex structure-activity relationship between its microstructure and catalytic performance. The traditional "trial-and-error" approach to developing new materials faces challenges such as long cycles and high costs. In recent years, the use of machine learning and artificial intelligence to assist in the design and optimization of g-C_3N_4 materials has opened up an efficient and precise new pathway for accelerating the development of high-performance photocatalysts by enabling performance prediction through big data analysis and inversely guiding synthesis. Wang Wentao et al. [66] systematically investigated 5d transition metals (5d TMs) doped intog-C_3N_4 as potential bifunctional OER/ORR electrocatalysts by considering defect charge states through defect chemistry studies. The results indicate that 33 types of 5d TM-doped g-CN exhibit improved stability under different charge states. Among them, Ir@CN (Ir occupying N sites), Ir@CN, Pt@CN (Pt occupying N sites), and Ir@CN (Ir at interstitial sites) demonstrated lower overpotentials, making them excellent candidates for bifunctional OER/ORR electrocatalysts. This is because modulating the charge states of 5d-TM@g-CN can adjust the interaction strength with oxygen-containing intermediates. Furthermore, machine learning revealed that the charge transfer (Q) and total magnetic moment (μ) of the TM atoms are the two most critical descriptors for OER and ORR overpotentials, respectively. The charged-defect tuning of bifunctional OER/ORR activity will advance the development of potential electrocatalysts for energy conversion applications.

7. Conclusions

This review first introduces the molecular structure and physicochemical properties of g-C_3N_4, exploring the fundamental principles of photocatalytic degradation of antibiotics. It summarizes the effects of different precursors and preparation methods on the morphology and functionality of carbon nitride. Finally, it discusses four methods—crystal structure optimization, element doping, surface modification, and heterojunction construction—along with practical case studies that illustrate how to enhance the capability of g-C_3N_4 in catalyzing antibiotic degradation. Among these, the construction of heterojunctions has garnered significant interest from researchers.

Machine learning and artificial intelligence technologies are revolutionizing the rational design of catalysts, significantly overcoming the high cost and low efficiency bottlenecks associated with traditional trial-and-error approaches. This methodology generally follows a closed-loop workflow: First, a standardized database containing catalyst composition, structural features (e.g., specific surface area, bandgap), and catalytic performance (e.g., degradation efficiency, conversion rate) is constructed from literature and experimental data. Subsequently, various machine learning models (such as Random Forest, Support

Vector Machines, or Neural Networks) are trained using this database to learn the complex non-linear relationships between descriptors (e.g., elemental electronegativity, atomic radius, synthesis conditions) and the target properties. A successfully trained model can rapidly predict the catalytic activity of unknown combinations and, inversely, recommend new candidate materials with optimal performance. For instance, by analyzing the performance data of known g-C_3N_4-based heterojunctions, the model can accurately predict which metal element doping or which semiconductor coupling most effectively promotes charge separation and narrows the bandgap, thereby achieving efficient degradation of specific antibiotics (e.g., tetracycline). This approach not only shortens the new material development cycle from years to weeks but also reveals hidden structure-activity relationships, guiding the synthesis of novel high-efficiency catalysts that surpass conventional empirical knowledge. Although challenges such as data quality and model interpretability remain, artificial intelligence has undoubtedly become a key driver in accelerating the discovery and optimization of advanced photocatalysts.

As a novel photocatalytic material, g-C_3N_4 demonstrates promising potential for antibiotic degradation. Its excellent visible light responsiveness and physicochemical properties offer effective solutions for antibiotic removal. Researchers have significantly improved the capability of g-C_3N_4 to generate photogenerated charge carriers, resulting in notable effectiveness in treating antibiotics in complex water bodies. However, the practical application of g-C_3N_4 in antibiotic degradation still faces a series of technical bottlenecks. Firstly, there is a lack of novel photoreactor designs capable of ensuring large-area uniform illumination and efficient mass transfer. Secondly, the limited light penetration in high-concentration wastewater leads to low photon utilization efficiency. Finally, it remains challenging to maintain the structural stability and catalytic activity of g-C_3N_4-based catalysts under long-term continuous operation. Therefore, future research should focus on addressing these engineering challenges to achieve efficient and scalable antibiotic degradation.

Author Contributions: X.L. contributed to conceptualization, data curation, investigation, and writing—original draft. D.C. contributed to investigation. J.W. contributed to investigation. S.G. contributed to investigation. Y.Z. contributed to investigation. S.L. contributed to conceptualization. Assoc. J.Y. contributed to data curation. M.Z. contributed to investigation, writing—review & editing, and supervision. J.M. contributed to visualization, writing—review & editing, and supervision. All authors have read and agreed to the published version of the manuscript.

Funding: This research is partially based on the works of the Center for Collaborative Innovation in the Heritage and Development of Xizang Culture (XT-ZB202531), National Key R&D Program of China (Grant No. 2022 YFC 3203304), the National Natural Science Foundation of China (52170153, 51708295), the Key Research and Development Program of Xizang (XZ202301ZY0031G), Young Scholar Incubation Plan of Xizang Minzu University (25MDQ05, 25MDX03) and the Science and Technology Innovation Project on Emission Peak and Carbon Neutrality of Jiangsu Province (BK20220038).

Data Availability Statement: The data that support the findings of this study are available from the corresponding author upon reasonable request.

Conflicts of Interest: The authors declare no conflict of interest.

References

1. Antos, J.; Piosik, M.; Ginter-Kramarczyk, D.; Zembrzuska, J.; Kruszelnicka, I. Tetracyclines Contamination in European Aquatic Environments: A Comprehensive Review of Occurrence, Fate, and Removal Techniques. *Chemosphere* **2024**, *353*, 141519. [CrossRef]
2. Zhu, M.-C.; Lu, Y.-Z.; Chen, S.-W.; Hu, Z.-X.; Wang, J.-W.; Li, N.; Zeng, R.J.-X. Carbon Nano-Onions Acting as Artificial Pili Enhance Chloramphenicol Degradation in an Anaerobic Membrane Bioreactor. *Chem. Eng. J.* **2023**, *475*, 146110. [CrossRef]

3. Işıtan, A. Sustainable Adsorption of Amoxicillin and Sulfamethoxazole onto Activated Carbon Derived from Food and Agricultural Waste: Isotherm Modeling and Characterization. *Processes* **2025**, *13*, 2528. [CrossRef]
4. Adamek, E.; Baran, W. Degradation of Veterinary Antibiotics by the Ozonation Process: Product Identification and Ecotoxicity Assessment. *J. Hazard. Mater.* **2024**, *469*, 134026. [CrossRef] [PubMed]
5. Li, Y.; Zhang, C.; Zhao, G.; Su, P.; Wang, J.; Li, Y.; Zhou, W.; Mu, Y.; Zhang, J.; Liu, W. A Critical Review on Antibiotics Removal by Persulfate-Based Oxidation: Activation Methods, Catalysts, Oxidative Species, and Degradation Routes. *Process. Saf. Environ. Prot.* **2024**, *187*, 622–643. [CrossRef]
6. Phuong, N.M.; Hai, P.V.; Viet, N.M.; Pham, T.-D.; Ha, T.T.V.; Hoang, D.H.; Minh, D.N.; Noi, N.V.; Rene, E.R.; Minh, T.D. Synthesis and Characterization of Z-Scheme Heterojunction $CoWO_4$/RGO/g-C_3N_4 as a Visible Light-Driven Photocatalyst for Novel Removal of Organic Pollutant. *J. Environ. Eng.* **2023**, *149*, 04022098. [CrossRef]
7. Liu, W.; Hui, J.; Cheng, X.; Zhang, L.; Li, Y.; Li, C.; Qi, C. Experimental Study on the Activation Energy of Coal Oxidation Under Different Oxygen Concentrations. *Processes* **2025**, *13*, 2889. [CrossRef]
8. Zhao, B.; Zhong, W.; Chen, F.; Wang, P.; Bie, C.; Yu, H. High-Crystalline g-C_3N_4 Photocatalysts: Synthesis, Structure Modulation, and H_2-Evolution Application. *Chin. J. Catal.* **2023**, *52*, 127–143. [CrossRef]
9. Roy, R.; Chacko, A.R.; Abraham, T.; Korah, B.K.; John, B.K.; Punnoose, M.S.; Mohan, C.; Mathew, B. Recent Advances in Graphitic Carbon Nitrides (g-C_3N_4) as Photoluminescence Sensing Probe: A Review. *ChemistrySelect* **2022**, *7*, e202200876. [CrossRef]
10. Dai, C.; Feng, Z.; Hu, Q.; Qiu, J.; You, J.; Guo, R.; Liu, X.; Zhang, H. Recent Progress in Modification and Composite Strategies of Graphitic Carbon Nitride as Catalysts for Heterogeneous Photo-Fenton Reaction. *Mater. Sci. Semicond. Process.* **2023**, *167*, 107807. [CrossRef]
11. Moeinifard, B.; Najafi Chermahini, A. Fabrication of Au-Doped Mesoporous TiO_2 Supported on g-C_3N_4 as an Efficient Light-Assisted Catalyst for Oxidative Desulfurization of Model Fuels with Different Sulfur Content. *Int. J. Mech. Mater. Eng.* **2025**, *20*, 14. [CrossRef]
12. Ya, Z.; Zhang, S.; Xu, D.; Wang, H.; Li, M. Coupling Plastic Upgrading and Photocatalysis: Catalytic Mechanisms and Design Principles. *ACS Catal.* **2025**, *15*, 5339–5369. [CrossRef]
13. Zhang, Z.; Liang, J.; Zhang, W.; Zhou, M.; Zhu, X.; Liu, Z.; Li, Y.; Guan, Z.; Lee, C.-S.; Wong, P.K.; et al. Modified-Pollen Confined Hybrid System: A Promising Union for Visible-Light-Driven Photocatalytic Antibiotic Degradation. *Appl. Catal. B Environ. Energy* **2023**, *330*, 122621. [CrossRef]
14. Chand, H.; Kumar, A.; Goswami, S.; Krishnan, V. Comparison of Catalytic Activity of Graphitic Carbon Nitrides Derived from Different Precursors for Carbon Dioxide Conversion. *Fuel* **2023**, *357*, 129757. [CrossRef]
15. Yu, Q.; Ren, X.; Pan, J.; Wang, Q.; Li, Y.; Shi, N. Chemical Bonds in Precursors Regulate G-C_3N_4 Structure and Its Photocatalytic Performance. *J. Alloys Compd.* **2022**, *910*, 164953. [CrossRef]
16. Chamorro-Posada, P.; Dante, R.C.; Vázquez-Cabo, J.; Dante, D.G.; Martín-Ramos, P.; Rubiños-López, Ó.; Sánchez-Arévalo, F.M. From Urea to Melamine Cyanurate: Study of a Class of Thermal Condensation Routes for the Preparation of Graphitic Carbon Nitride. *J. Solid State Chem.* **2022**, *310*, 123071. [CrossRef]
17. Zheng, H.; Chen, Y.; Sun, X.; Zheng, X.; Zhang, X.; Guan, X. Enhanced Photocatalytic Performance and Mechanism of N-Deficiently Porous g-C_3N_4 in Organic Pollutant Degradation. *Mater. Res. Bull.* **2023**, *169*, 112510. [CrossRef]
18. Ba, G.; Hu, H.; Bi, F.; Yu, J.; Liu, E.; Ye, J.; Wang, D. Engineering Nitrogen Vacancies and Cyano Groups into C_3N_4 Nanosheets for Highly Efficient Photocatalytic H_2O_2 Production. *Appl. Catal. B Environ. Energy* **2024**, *361*, 124645. [CrossRef]
19. Lei, S.; Wang, W.; Wang, C.; Li, W.; Xu, Z.; Li, G.; An, T. Photo-Transformation of Graphitic Carbon Nitride Synthesized from Different Precursors: Influence on Environmental Fate and Photocatalytic Water Disinfection. *J. Water Process Eng.* **2024**, *61*, 105279. [CrossRef]
20. Torres-Pinto, A.; Silva, C.G.; Faria, J.L.; Silva, A.M.T. The Effect of Precursor Selection on the Microwave-Assisted Synthesis of Graphitic Carbon Nitride. *Catal. Today* **2022**, *424*, 113868. [CrossRef]
21. Zhai, Y.; Lv, L.; Fan, J. Synthesis of CuO/$ZnWO_4$ Heterojunction Structure for H_2S Gas Sensor with Ultra-High Response Value at Room Temperature. *Processes* **2025**, *13*, 2727. [CrossRef]
22. Kailasam, K.; Epping, J.D.; Thomas, A.; Losse, S.; Junge, H. Mesoporous Carbon Nitride–Silica Composites by a Combined Sol–Gel/Thermal Condensation Approach and Their Application as Photocatalysts. *Energy Environ. Sci.* **2011**, *4*, 4668. [CrossRef]
23. Muhmood, T.; Uddin, A. Fabrication of Spherical-Graphitic Carbon Nitride via Hydrothermal Method for Enhanced Photo-Degradation Ability towards Antibiotic. *Chem. Phys. Lett.* **2020**, *753*, 137604. [CrossRef]
24. Wu, X.; Fan, H.; Wang, W.; Lei, L.; Chang, X. Ordered and Ultralong Graphitic Carbon Nitride Nanotubes Obtained via In-Air CVD for Enhanced Photocatalytic Hydrogen Evolution. *ACS Appl. Energy Mater.* **2021**, *4*, 13263–13271. [CrossRef]
25. Zhou, Y.; Zhang, Y.; Xue, J.; Wang, R.; Dong, J.; Yin, Z.; Guo, C.; Wang, H. Electrochemically Assisted Preparation of Graphitic Carbon Nitride Nanosheet Membranes for Efficient Water Purification. *Chem. Eng. J.* **2024**, *490*, 151638. [CrossRef]
26. Kamble, G.; Ganai, A.M.; Lakshmi, D.V.; Rao, N.N.; Rajarikam, N.; Rao, P.V. Impact of Pyrolysis Temperature on Physicochemical Properties of Carbon Nitride Photocatalyst. *Semicond. Sci. Technol.* **2023**, *36*, 055020. [CrossRef]

27. Shenoy, S.; Chuaicham, C.; Sekar, K.; Sasaki, K. Seamless Carbon Nitride Growth on Bimetallic Oxide for Antibiotic Residue Degradation. *Environ. Chem. Lett.* **2024**, *23*, 33–39. [CrossRef]
28. Zhou, Y.; Jiang, D.; Wang, Z.; Yi, L.; Sun, J.; Liu, D.; Yu, X.; Chen, Y. Bandgap Engineering of Carbon Nitride by Formic Acid Assisted Thermal Treatment for Photocatalytic Degradation of Tetracycline Hydrochloride. *Chem. Eng. J.* **2024**, *485*, 149830. [CrossRef]
29. Xiao, Y.; Geng, A.; Zhu, J.; Xu, X.; Xu, X. Metal Doped Graphitic Carbon Nitride Prepared by a Bubbling Template Method for Photo-Degradation of Organic Pollutants. *J. Phys. Appl. Phys.* **2022**, *55*, 434002. [CrossRef]
30. Wu, L.; Lu, Z.; Liao, J.; Xiang, X.; Song, H.; Yang, A.; Ibupoto, Z.H.; Lv, K. Photocatalytic Degradation of Sulfonamides in Suspensions of Coral-like Graphene Carbon Nitride with Nitrogen Vacancies. *Chemosphere* **2024**, *352*, 141313. [CrossRef]
31. Mohamed, H.H.; Aziz, M.; Youssef, T.E.; Alomair, N.A. Microwave Synthesized G-C_3N_4 Nanofibers with Modified Properties for Enhanced Solar Light Photocatalytic Performance. *Inorg. Chem. Commun.* **2024**, *168*, 112975. [CrossRef]
32. Li, P. The Study of G-C_3N_4 with Modified Precursor Prepared by Microwave and Its Properties. Master's Thesis, Tianjin University of Science and Technology, Tianjin, China, 2024.
33. Briševac, D.; Gabelica, I.; Radovanović-Perić, F.; Tolić Čop, K.; Matijašić, G.; Ljubas, D.; Ćurković, L. Influence of Different Precursors on Properties and Photocatalytic Activity of G-C_3N_4 Synthesized via Thermal Polymerization. *Materials* **2025**, *18*, 2522. [CrossRef]
34. Latif, M.J.; Ali, S.; Jamil, S.; Bibi, S.; Jafar, T.; Rasheed, A.; Noreen, S.; Bashir, A.; Rauf Khan, S. Comparative Catalytic Reduction and Degradation with Biodegradable Sodium Alginate Based Nanocomposite: Zinc Oxide/N-Doped Carbon Nitride/Sodium Alginate. *Int. J. Biol. Macromol.* **2023**, *254*, 127954. [CrossRef] [PubMed]
35. Medina-Llamas, M.; Bianchi, E.; Mozzati, M.C.; Tedesco, C.; Milanese, C.; Speltini, A.; Profumo, A.; Armenise, V.; Milella, A.; Listorti, A.; et al. Synthesis of Carbon Nitride Polymorphs by Sacrificial Template Method: Correlation between Physicochemical Properties and Photocatalytic Performance. *ChemSusChem* **2024**, *18*, e202400918. [CrossRef] [PubMed]
36. Tang, Q.; Zhang, Z.; Pan, Y.; Leung, M.K.H.; Zhang, Y.; Chen, K. Carbon Nitride Gels: Synthesis, Modification, and Water Decontamination Applications. *Gels* **2025**, *11*, 685. [CrossRef] [PubMed]
37. Guo, L.; Gao, J.; Huang, Q.; Wang, X.; Li, Z.; Li, M.; Zhou, W. Element Engineering in Graphitic Carbon Nitride Photocatalysts. *Renew. Sustain. Energy Rev.* **2024**, *199*, 114482. [CrossRef]
38. Li, X.; Wu, J.; An, S.; Li, K.; Zhang, J.; Pei, M.; Song, C.; Guo, X. Ultrathin Crystalline Carbon Nitride Nanosheets for Highly Efficient Photocatalytic Pollutant Removal and Hydrogen Production. *ACS Appl. Nano Mater.* **2023**, *6*, 11601–11611. [CrossRef]
39. Zhang, J.; Li, Y.; Gong, Y.; Zhu, C.; Zhang, L.; Tang, H.; He, W.; Wang, B. Bi(III) and Ce(IV) Functionalized Carbon Nitride Photocatalyst for Antibiotic Degradation: Synthesis, Toxicity, and Mechanism Investigations. *Chemosphere* **2023**, *333*, 138888. [CrossRef]
40. Yuan, A.; Lei, H.; Xi, F.; Liu, J.; Qin, L.; Chen, Z.; Dong, X. Graphene Quantum Dots Decorated Graphitic Carbon Nitride Nanorods for Photocatalytic Removal of Antibiotics. *J. Colloid Interface Sci.* **2019**, *548*, 56–65. [CrossRef]
41. Zhang, X.; Xu, X.; Li, C.; Dai, L.; Hao, Z.; Yu, J.; He, H.; Si, C.; Shen, Z.; Qiu, Z.; et al. Metal-Free Graphitic Carbon Nitride/Black Phosphorus Quantum Dots Heterojunction Photocatalyst for the Removal of ARG Contamination. *Adv. Compos. Hybrid Mater.* **2023**, *6*, 145. [CrossRef]
42. Yang, L.; Wang, F.; Hakki, A.; Macphee, D.E.; Liu, P.; Hu, S. The Influence of Zeolites Fly Ash Bead/TiO_2 Composite Material Surface Morphologies on Their Adsorption and Photocatalytic Performance. *Appl. Surf. Sci.* **2017**, *392*, 687–696. [CrossRef]
43. Wang, K.; Shu, Z.; Zhou, J.; Zhao, Z.; Wen, Y.; Sun, S. Enhancing Piezocatalytic H_2O_2 Production through Morphology Control of Graphitic Carbon Nitride. *J. Colloid Interface Sci.* **2023**, *648*, 242–250. [CrossRef]
44. Pattanayak, D.S.; Thakur, C.; Pal, D. Synthesis of Exfoliated Graphitic Carbon Nitride (g-C_3N_4) for Tetracycline Hydrochloride (TCH) Degradation: Photocatalytic Efficiency and Mechanisms. *Arab. J. Sci. Eng.* **2025**, *50*, 10039–10050. [CrossRef]
45. Zhan, X.; Zeng, Y.; Zhang, H.; Wang, X.; Jin, D.; Jin, H.; Luo, S.; Yang, L.; Hong, B. The Coral-like Carbon Nitride Array: Rational Design for Efficient Photodegradation of Tetracycline under Visible Light. *J. Environ. Chem. Eng.* **2022**, *11*, 109201. [CrossRef]
46. Oh, W.-D.; Chang, V.W.C.; Hu, Z.-T.; Goei, R.; Lim, T.-T. Enhancing the Catalytic Activity of G-C_3N_4 through Me Doping (Me = Cu, Co and Fe) for Selective Sulfathiazole Degradation via Redox-Based Advanced Oxidation Process. *Chem. Eng. J.* **2017**, *323*, 260–269. [CrossRef]
47. Li, J.; Liu, H.; Bai, X.; Rao, X.; Zhang, Y. N, S-Doped Graphene Quantum Dots Grafted Graphitic Carbon Nitride to Boost Its Photocatalytic Hydrogen Evolution and Antibacterial Activity. *Nano* **2022**, *17*, 2250066. [CrossRef]
48. Singh, S.; Singhal, R.; Yadav, R.K.; Gupta, N.K. In-Situ 'X' Doped 'GCN' Photocatalyst Enables Selective Aldehyde Synthesis via Photo-Oxidation of Benzyl Alcohol under Ambient Conditions. *Diam. Relat. Mater.* **2024**, *149*, 111609. [CrossRef]
49. Zeng, Y.; Wu, L.; Luo, J.; Lu, X.; Jia, B.; Liang, L.; Zhang, J. Photocatalytic Degradation of Ciprofloxacin by Gd-Co/g-C_3N_4 under Low-Power Light Source: Degradation Pathways and Mechanistic Insights. *J. Water Process Eng.* **2024**, *58*, 104849. [CrossRef]

50. Kong, Y.; Li, D.; Zhang, C.; Han, W.; Xue, Y.; Zhang, W.; Sun, H.; Wang, S.; Duan, X. Synergistic Silver Doping and N Vacancy Promoting Photocatalytic Performances of Carbon Nitride for Pollutant Oxidation and Hydrogen Production. *Chem. Eng. J.* **2023**, *479*, 147676. [CrossRef]
51. Bhoyar, T.; Saraswat, N.; Jyothirmai, M.V.; Gupta, A.; Malla, S.K.; Park, J.; Vidyasagar, D.; Umare, S.S. Nitrogen-Doped Graphitic Carbon Dots Embedded in Carbon Nitride Scaffolds for Water Decontamination. *ACS Appl. Nano Mater.* **2023**, *6*, 3484–3496. [CrossRef]
52. Gan, J.; Ma, X.; Qi, X.; Qin, Q.; Gong, Y.; Han, J.; Jin, T. Sunlight-Induced Multifunctional Photocatalyst of Gold-Deposited Graphitic Carbon Nitride with Enhanced Efficiency of Antibacterial, Antiviral, and Antibiotic Degradation. *J. Environ. Chem. Eng.* **2023**, *12*, 111810. [CrossRef]
53. Zhao, Y.; Wang, S.; Sun, Z.; Liu, Q.; Ma, J. Carbon Quantum Dot Implanted Graphite Carbon Nitride Nanorod with Enhanced Photocatalytic Activity: Mechanisms, Degradation Pathway and DFT Calculation. *Mater. Sci. Semicond. Process.* **2023**, *172*, 108056. [CrossRef]
54. Deng, A.; Sun, Y.; Gao, Z.; Yang, S.; Liu, Y.; He, H.; Zhang, J.; Liu, S.; Sun, H.; Wang, S. Internal Electric Field in Carbon Nitride-Based Heterojunctions for Photocatalysis. *Nano Energy* **2023**, *108*, 108228. [CrossRef]
55. Lei, Y.; Ye, J.; García-Antón, J.; Liu, H. Recent Advances in the Built-in Electric-Field-Assisted Photocatalytic Dry Reforming of Methane. *Chin. J. Catal.* **2023**, *53*, 72–101. [CrossRef]
56. Xu, Y.; Hou, W.; Huang, K.; Guo, H.; Wang, Z.; Lian, C.; Zhang, J.; Wu, D.; Lei, Z.; Liu, Z.; et al. Engineering Built-In Electric Field Microenvironment of CQDs/g-C_3N_4 Heterojunction for Efficient Photocatalytic CO_2 Reduction. *Adv. Sci.* **2024**, *11*, 2403607. [CrossRef]
57. Dong, J.; Zhao, J.; Yan, X.; Li, L.; Liu, G.; Ji, M.; Wang, B.; She, Y.; Li, H.; Xia, J. Construction of Carbonized Polymer Dots/Potassium Doped Carbon Nitride Nanosheets Van Der Waals Heterojunction by Ball Milling Method for Facilitating Photocatalytic CO_2 Reduction Performance in Pure Water. *Appl. Catal. B Environ. Energy* **2024**, *351*, 123993.
58. Tofaz, T.; Lu, X.-J.; Chen, S.; Li, J.-H.; Ding, H.-Y.; Ullah, I.; Habib, S.; Murtaza, G.; Xu, A.-W. 4,4′,4″-Nitrilotribenzoic Acid/Graphitic Carbon Nitride Type II Heterostructures for Highly Efficient Photocatalytic Hydrogen Evolution from Water Splitting. *ACS Appl. Energy Mater.* **2024**, *7*, 12016–12026. [CrossRef]
59. Ramos Corona, A.; Rodríguez López, J.; Rangel Segura, R.; Martínez Garcia, M.M.; Flores, E.; Rodríguez Gattorno, G.; Alvarado Gil, J.J. Microwave-Assisted Synthesis of CdS-MOF MIL-101 (Fe) Composite: Characterization and Photocatalytic Performance. *Inorg. Chem.* **2024**, *63*, 19536–19552. [CrossRef]
60. Malefane, M.E.; Mafa, P.J.; Managa, M.; Nkambule, T.T.I.; Kuvarega, A.T. Understanding the Principles and Applications of Dual Z-Scheme Heterojunctions: How Far Can We Go? *J. Phys. Chem. Lett.* **2023**, *14*, 1029–1045. [CrossRef] [PubMed]
61. Zhao, D.; Yang, Y.; Binas, V.; Shen, S. Interface Engineering of Z-Scheme Heterojunction for Photocatalytic Water Splitting. *Fundam. Res.* **2024**, *5*, 2204–2208. [CrossRef]
62. Dang, J.; Zhang, J.; Shen, Y.; Wang, L.; Guo, F.; Li, Y.; Guan, W. Fabrication of Magnetically Recyclable Fe_3O_4/BiOCl/BiOBr Nanocomposite with Z-Scheme Heterojunction for High-Efficiency Photocatalytic Degradation of Tetracycline. *Mater. Sci. Semicond. Process.* **2023**, *158*, 107371. [CrossRef]
63. Zhang, X.; Chen, H.; Liu, S.; Zhang, B.; Zhu, H.; Chen, H.; Wen, B.; Chen, L. Preparation of TiO_2-Graphitized Carbon Composite Photocatalyst and Their Degradation Properties for Tetracycline Antibiotics. *J. Mol. Struct.* **2022**, *1270*, 133897. [CrossRef]
64. Zhou, H.; Cui, J.; Pang, L.; Wangjin, Y.; Li, M.; Zhao, Z.; Huang, L. Removal of Antibiotics and Antibiotic Resistance Genes from Urban Rivers Using a Photocatalytic-and-Bionic Artificial Ecosystem. *J. Clean. Prod.* **2022**, *348*, 131311. [CrossRef]
65. Rapti, I.; Boti, V.; Albanis, T.; Konstantinou, I. Photocatalytic Degradation of Psychiatric Pharmaceuticals in Hospital WWTP Secondary Effluents Using G-C_3N_4 and g-C_3N_4/MoS_2 Catalysts in Laboratory-Scale Pilot. *Catalysts* **2023**, *13*, 252. [CrossRef]
66. Wang, W.; Qu, Y.; Li, D.; Zhang, A.; Yan, H.; Feng, Z.; Yao, W. The Defect Chemistry and Machine Learning Study 5d Transition Metal Doped on Graphitic Carbon Nitride for Bifunctional Oxygen Electrocatalyst with Low Overpotential. *Int. J. Hydrogen Energy* **2024**, *79*, 702–714. [CrossRef]

Disclaimer/Publisher's Note: The statements, opinions and data contained in all publications are solely those of the individual author(s) and contributor(s) and not of MDPI and/or the editor(s). MDPI and/or the editor(s) disclaim responsibility for any injury to people or property resulting from any ideas, methods, instructions or products referred to in the content.